Scheme I

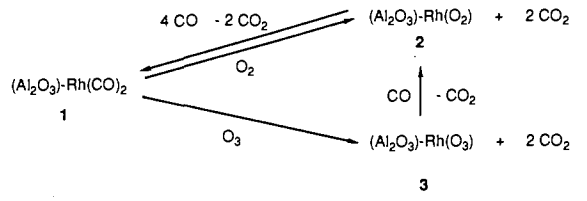

Scheme II

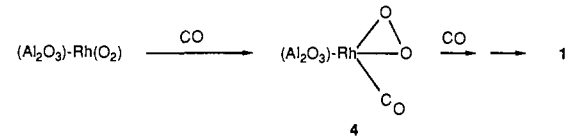

conditions to dioxygen or ozone adducts using O_2 or O_3, respectively. We believe the latter compound to be the first example of an ozone complex prepared and stable under ambient conditions.[4]

Reaction between an octane solution of (allyl)$Rh(CO)_2$ and alumina or between a toluene solution of $(allyl)_3Rh$ and alumina followed by carbonylation gives bound, mononuclear rhodium dicarbonyl compound **1**.[5] When this material was treated in a stream of dry O_2 (1 atm, 140 °C, 500 h), the characteristic metal dicarbonyl infrared absorption at 2060 and 2090 cm^{-1} was lost resulting in a spectrum for **2** which is featureless in the region 3000–1000 cm^{-1}, and which was masked by oxide absorption below that energy. Similar infrared results were obtained when **1** was treated with dry ozone (1% in O_2, 25 °C, 5 h) to give **3**. X-ray photoelectron spectroscopy was performed on **2** and **3** to assign them as oxidized rhodium compounds.[6] In this way, binding energies for Rh $3d_{5/2}$ = 309.0 and 310.0 eV (vs C 1s = 284.3 eV) were obtained for **2** and **3**, respectively. (For comparison, Rh_2O_3 $3d_{5/2}$ = 309.1 eV;[7] for **1**, 308.9 eV; for Rh(metal)/Al_2O_3, 307.5 eV.[8]) Treating either **2** or **3** with CO regenerated **1**, and quantitative analysis of the oxidation of **1**, or recarbonylation of **2** or **3** confirms the stoichiometries of these materials as O_2 and O_3 adducts, respectively. For example, **2** reacted with CO in a closed system by sequential CO addition at 20–30 mm at 120 °C for a total reaction time of 466 h to give 2 equiv of CO_2. An additional 2 equiv of CO were absorbed to regenerate **1**. A similar procedure with **3** gave 3 equiv of CO_2 and **1** (a net uptake of 5 equiv of CO).[9] In this latter study it was found that 1 equiv of CO_2 was produced rapidly, but the next 2 equiv of CO_2 were produced slowly (Scheme I).

The oxidation of CO by **2** was studied through sequential addition of fractional equivalent amounts of CO.[10] An intermediate carbonyl compound (**4**) was obtained (ν_{CO} = 2100 cm^{-1}). Under these conditions (118 °C, ~0.4 mm p_{CO}, 1 h), uptake of up to 1 equiv of CO occurs with no measurable CO_2 production. When quantities exceeding 1 equiv of CO were used, CO_2 production was observed. We believe that oxidation of CO occurs as shown in Scheme II.

Consistent with the interconversions shown in Scheme I, it was found that **2** would catalyze oxidation of CO to CO_2 by O_2. Under a variety of conditions tested, rates for oxidation of CO catalyzed by these materials which are prepared by specified organometallic deposition routes, compare favorably with results obtained for likely similar (carbonyl) compounds formed by inorganic impregnation, reduction, and carbonylation procedures.[11] (Indeed compounds observed in situ for CO oxidation by these latter species[11] may be **2** and **4**.) Analogues of **2** and **3** were prepared on titania or silica (XPS: for TiO_2–**3**, 311.0 eV; for SiO_2–**2**, 310.0 eV[12]). Oxidation of CO catalyzed by these materials occurs at different relative rates depending on the $CO:O_2$ ratio. Thus when $CO:O_2$ = 5 (the "resting species" is likely **1**[13]) relative rates for CO_2 production are 1.84:1.1:1 for titania-, silica-, and alumina-supported materials, respectively, while for $CO:O_2$ = 0.54 (the "resting species" likely also contains **4**[14]), rates are 9.2:2.1:1. These small but real differences in reactivity may be due to different geometrical requirements for oxide ligand coordination afforded by the various oxides to the rhodium complexes in their reduced (**1**) or oxidized (**2**) forms. Detailed structural investigations of **2** and **3** are now underway, as are examinations of reactivity of these materials with organic substrates.

Acknowledgment. We acknowledge support for this research provided by the Gas Research Institute and the National Science Foundation. We also thank Dr. Dennis Anderson, Englehardt Industries, for XPS data.

(4) Ionic ozonides prepared and studied in argon or nitrogen matrices are well-known. See: Prochaska, E. S.; Andrews, L. *J. Chem. Phys.* **1980**, *72*, 6782.

(5) McNulty, G. S.; Cannon, K.; Schwartz, J. *Inorg. Chem.* **1986**, *25*, 2919.

(6) For a range of values, see: Andersson, S. L. T.; Watters, K. L.; Howe, R. F. *J. Catal.* **1981**, *69*, 212.

(7) Contour, J. P.; Mouvier, G.; Hoogewij, S. M.; Leclerc, L. *J. Catal.* **1977**, *48*, 217.

(8) Huizinga, T.; van't Blik, H. F. J.; Vis, J. C.; Prins, R. *Surf. Sci.* **1983**, *135*, 580.

(9) Stoichiometries of these complexes were determined by subjecting a weighed amount of each to a series of aliquots of CO in a closed system at 120 °C. Species **2** was given 14 aliquots of CO (20–30 mmHg, ~8 equiv per Rh) for 12–80 h. At the end of each period the system was assayed for CO_2 content by GC. The reaction was judged to be complete when 80 hours had elapsed with no further detectable conversion. A similar procedure was used with **3**.

(10) Complex **2** was treated with fractional equivalents of CO (0.1–0.3 equiv of CO/Rh, ~0.4 mm p_{CO}) at 118 °C for short periods (~1 h).

(11) For example, see: Kiss, J. T.; Gonzalez, R. D. *J. Phys. Chem.* **1984**, *88*, 898.

(12) Cannon, K. C.; Jo, S. K.; White, J. M. private communication.

(13) Under these conditions (95 °C, p_{CO} = 30 mm, p_{O_2} = 6 mm), determined in situ, ν_{CO} = 2100, 2030 cm^{-1} for the Al_2O_3-bound material. Rates for CO oxidation are as follows: (TiO_2) 1.15 × 10^{-5} equiv/s; (SiO_2) 6.8 × 10^{-6} equiv/s; (Al_2O_3) 6.3 × 10^{-6} equiv/s.

(14) Under these conditions (95 °C, p_{CO} = 10 mm, p_{O_2} = 18.5 mm), determined in situ, ν_{CO} = 2138 (sh), 2100, 2030 cm^{-1} for the Al_2O_3-bound material. Rates for CO oxidation are as follows: (TiO_2) 4.73 × 10^{-5} equiv/s; (SiO_2) 1.06 × 10^{-5} equiv/s; (Al_2O_3) 5.2 × 10^{-6} equiv/s.

Ferromagnetic Coupling via Imidazolate in an Iron(III)–Porphyrin–Dicopper(II) System

Carol A. Koch and Christopher A. Reed*

Department of Chemistry
University of Southern California
Los Angeles, California 90089-0744

Greg A. Brewer*

Department of Chemistry
The Catholic University of America
Washington, D.C. 20064

Nigam P. Rath and W. Robert Scheidt*

Department of Chemistry
University of Notre Dame
Notre Dame, Indiana 46556

Govind Gupta and George Lang*

Department of Physics
Pennsylvania State University
University Park, Pennsylvania 16802

Received April 17, 1989

The demonstrated,[1] postulated,[2] or possible[3] existence of histidine-derived imidazolate bridging ligands in multimetal proteins

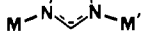

(1) In bovine superoxide dismutase: Tainer, J. A.; Getzoff, E. D.; Beem, K. M.; Richardson, J. S.; Richardson, D. C. *J. Mol. Biol.* **1982**, *160*, 181.

0002-7863/89/1511-7645$01.50/0

has stimulated considerable investigation into the role of imidazolate as a mediator of magnetic coupling. Without exception, the magnetically coupled systems explored to date have displayed *antiferro*magnetic coupling, and the focus of study has been in establishing its magnitude and mechanism.[4-13] Herein, we report the first example of *ferro*magnetic coupling via imidazolate bridging ligands. It was discovered in a trinuclear $S = {}^1/_2$, $S = {}^1/_2$, $S = {}^1/_2$ system which utilizes a copper(II) imidazolate complex for bis axial ligation to a low-spin iron(III) porphyrin. Ferromagnetically coupled heterotrinuclear systems are very rare,[14] and few trinuclear systems[15] have a clear origin of their ferromagnetic interaction.

The ability of the copper(II) and nickel(II) complexes of the Schiff base formed by sequential condensation of 5-chloro-2-hydroxybenzophenone, 1,2-diaminobenzene, and imidazole-4-carboxaldehyde, MIm, to act as imidazole-like ligands to iron porphyrins has been established by solution spectroscopic methods.[16] They are attractive components for magnetic interaction studies because each iron/copper system can be compared to an analogous iron/nickel "diamagnetic control" with the realistic expectation that comparisons are being made in isostructural pairs. The concept was first tested with iron(II) porphyrins where the Ni–Fe–Ni system was expected to give an all-diamagnetic trinuclear species and the Cu–Fe–Cu system was expected to give magnetically isolated copper(II) centers separated by diamagnetic iron(II). These expectations have been realized in the isolation from toluene solution of Fe(TPP)(NiIm)$_2$ and Fe(TPP)(CuIm)$_2$ (TPP = tetraphenylporphyrinate) whose UV–vis and Mossbauer spectra[17] closely match those of low-spin Fe(TPP)(HIm)$_2$ (HIm = imidazole). A small residual paramagnetism in Fe(TPP)(NiIm)$_2$ is ascribed to paramagnetic impurities (a common problem in this type of work). Fe(TPP)(CuIm)$_2$ behaves as a normal paramagnet with an essentially constant μ_{eff} value of 2.55 $\pm$ 0.05 μ_B from 300–10 K (attributed to two $S = 1/2$ ions with $g_{Cu} = 2.12$). The 10–2 K data indicate weak, pairwise antiferromagnetic coupling ($J_{CuCu} = -1.5$ cm^{-1}, $g = 2.12$ cm^{-1} for a $-JS_1S_2$ spin Hamiltonian) which may be of intra- or intermolecular origin (see below).

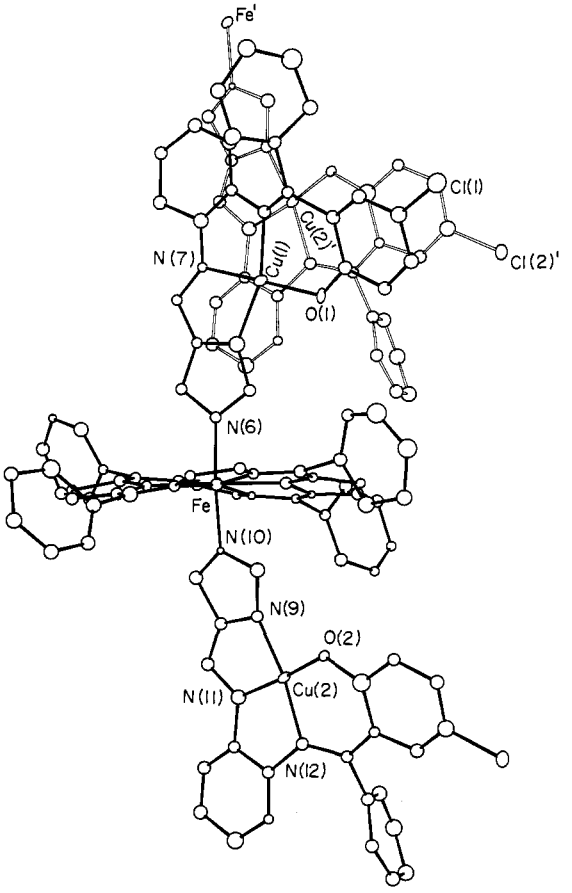

Figure 1. A perspective view of the cation in [Fe(TPP)(CuIm)$_2$]B$_{11}$CH$_{12}$·3DMF·3H$_2$O showing the two axial CuIm ligands. Also shown are the overlapping CuIm ligands in adjacent cations; the heavy and open bonds are related by a lattice translation. The two coordinated imidazolate planes form a dihedral angle of 20. Average distances in the porphyrin portion of the molecule are Fe–N_p = 2.00 (3) Å, Fe–N_{ax} = 1.98 (1) Å. Bond distances in the copper moieties are (average of two distances each) Cu–N_{im} = 1.98 (1) Å, Cu–N(11) = 1.92 (1) Å, Cu–N(12) 1.98 (1) Å, Cu–O = 1.86 (1) Å. The angles α and θ, defined in ref 11, are 174.9° and 7.4° at Cu(1) and 170.4° and 8.5° at Cu(2), respectively.

The chemistry of the iron(III) porphyrins was done with the large, weakly coordinating anion B$_{11}$CH$_{12}^-$ in order to minimize axial ligand competition and to aid crystallization. Treatment of Fe(TPP)(B$_{11}$CH$_{12}$)[18] with 2 equiv of NiIm or CuIm in tetrahydrofuran produced essentially quantitative yields of [Fe(TPP)(NiIm)$_2$]B$_{11}$CH$_{12}$·5THF and [Fe(TPP)(CuIm)$_2$]B$_{11}$CH$_{12}$·5THF. Their spectroscopic properties[19] closely match those of typical low-spin six-coordinate iron(III) porphyrins

(2) In cytochrome *c* oxidase: Palmer, G.; Babcock, G. T.; Vickery, L. E. *Proc. Natl. Acad. Sci. U.S.A.* **1976**, *23*, 2206.
(3) In magnetically coupled multiheme redox proteins: see, for example: (a) Anderson, K. K.; Lipscomb, J. D.; Valentine, M.; Munck, E.; Hooper, A. B. *J. Biol. Chem.* **1986**, *261*, 1126. (b) Blackmore, R. S.; Brittain, T.; Gadsby, P. M. A.; Greenwood, C.; Thompson, A. J. *FEBS Lett.* **1987**, *219*, 244.
(4) (a) Kolks, G.; Frihart, C. R.; Rabinowitz, H. N.; Lippard, S. J. *J. Am. Chem. Soc.* **1976**, *98*, 5720. (b) Strothkamp, K. G.; Lippard, S. J. *Acc. Chem. Res.* **1982**, *15*, 318.
(5) (a) Reed, C. A.; Landrum, J. T. *FEBS Lett.* **1979**, *106*, 265. (b) Landrum, J. T.; Grimmett, D.; Haller, K. J.; Scheidt, W. R.; Reed, C. A. *J. Am. Chem. Soc.* **1981**, *103*, 2640.
(6) Haddad, M. S.; Hendrickson, D. N. *Inorg. Chem.* **1978**, *17*, 2622.
(7) Hendriks, H. M. J.; Birker, P. J. M. W. L.; Verschoor, G. C.; Reedijk, J. *J. Chem. Soc., Dalton Trans.* **1982**, 623.
(8) Drew, M. G. B.; McCann, M.; Nelson, S. M *J. Chem. Soc., Dalton Trans.* **1981**, 1868.
(9) Morgenstern-Badarau, I.; Cocco, D.; Desideri, A.; Rotilio, G.; Jordanov, J.; Dupre, N. *J. Am. Chem. Soc.* **1986**, *108*, 300.
(10) Costes, J.-P.; Serra, J.-F.; Dahan, F.; Laurent, J.-P. *Inorg. Chem.* **1986**, *25*, 2790.
(11) Bencini, A.; Benelli, C.; Gatteschi, D.; Zanchini, C. *Inorg. Chem.* **1986**, *25*, 398.
(12) Brewer, G. A.; Sinn, E. *Inorg. Chem.* **1987**, *26*, 1529.
(13) Gross, R.; Kaim, W. *Inorg. Chem.* **1986**, *25*, 4865.
(14) (a) Bencini, A.; Benelli, C.; Caneschi, A.; Dei, A.; Gatteschi, D. *Inorg. Chem.* **1986**, *25*, 572. (b) Kahn, O. *Struct. Bonding* **1987**, *68*, 89.
(15) (a) Ginsberg, A. P.; Martin, R. L.; Sherwood, R. C. *Inorg. Chem.* **1968**, *7*, 932. (b) Kolks, G.; Lippard, S. J.; Waszczak, J. V. *J. Am. Chem. Soc.* **1980**, *102*, 4833. (c) Long, G. J.; Lindner, D.; Lintvedt, R. L.; Guthrie, J. W. *Inorg. Chem.* **1982**, *21*, 1431. (d) Gehring, S.; Astheimer, H.; Haase, W. *J. Chem. Soc., Faraday Trans.* **1987**, *83*, 347. (e) Gatteschi, D.; Laugier, J.; Rey, P.; Zanchini, C. *Inorg. Chem.* **1987**, *26*, 938.
(16) Brewer, C. T.; Brewer, G. A. *Inorg. Chem.* **1987**, *26*, 3420.
(17) Fe(TPP)(NiIm)$_2$·2toluene Anal. Calcd for $C_{90}H_{58}N_{12}O_2Cl_2FeNi_2$·$2C_7H_8$: C, 70.64; H, 4.23; N, 9.51; Fe, 3.20; Ni, 6.31. Found: C, 70.79; H, 4.40; N, 9.61; Fe, 3.16; Ni, 6.64. λ_{max}(toluene) 427 (Soret), 533, 565 nm; δ(Fe) 0.45, ΔE_Q 0.89 mm·s^{-1}. Fe(TPP)(CuIm)$_2$·2toluene Anal. Calcd for $C_{90}H_{58}N_{12}O_2Cl_2Cu_2Fe$·$2C_7H_8$: C, 70.26; H, 4.20; N, 9.46; Cu, 7.15; Fe, 3.14. Found: C, 70.04;, H, 4.41; N, 9.65; Cu, 7.11; Fe, 3.10. λ_{max}(toluene) 428 (Soret), 535, 566 nm; δ(Fe) 0.45, ΔE_Q 0.89 mm·s^{-1} at 4.2 K.
(18) Gupta, G. P.; Lang, G.; Lee, Y. J.; Scheidt, W. R.; Shelly, K.; Reed, C. A. *Inorg. Chem.* **1987**, *26*, 3022.
(19) [Fe(TPP)(NiIm)$_2$]B$_{11}$CH$_{12}$·5THF Anal. Calcd for $C_{91}H_{70}N_{12}O_2B_{11}Cl_2FeNi_2$·$5C_4H_8O$: C, 63.87; H, 5.31; N, 8.05; Fe, 2.68; Ni, 5.62. Found: C, 57.98; H, 4.97; N, 8.41; Fe, 2.95; Ni, 5.56. λ_{max}(THF) 417 (Soret), 549 nm; δ(Fe) 0.24, ΔE_Q 2.26 mm·s^{-1}. [Fe(TPP)(CuIm)$_2$]B$_{11}$CH$_{12}$·5THF Anal. Calcd for $C_{91}H_{70}N_{12}O_2B_{11}Cl_2FeCu_2$·$5C_4H_8O$: C, 63.57; H, 5.29; N, 8.02; Cu, 6.06; Fe, 2.67. Found: C, 63.28; H, 5.29; N, 8.08; Cu, 6.31; Fe, 2.47. λ_{max}(THF) 417 (Soret), 549 nm; δ(Fe) 0.23; ΔE_Q 2.07 mm·s^{-1} at 4.2 K.

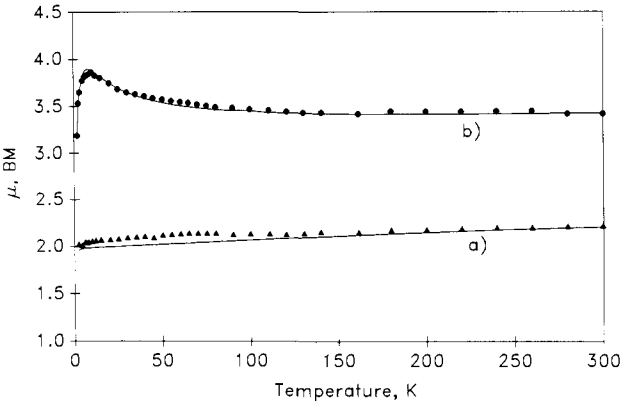

Figure 2. Magnetic moment per trinuclear unit versus temperature for (a) $[Fe(TPP)(NiIm)_2]B_{11}CH_{12}\cdot 5THF$ and (b) $[Fe(TPP)(CuIm)_2]B_{11}CH_{12}\cdot 5THF$. Solid lines are theoretical fits as described in the text.

such as $[Fe(TPP)(HIm)_2]^+$, and the structure of the most interesting of these complexes has been established by X-ray crystallography.[20] Figure 1 shows how the essentially square-planar CuIm complexes act as axial ligands to the $Fe^{III}(TPP)$ cation via imidazolate bridges. The coordinate geometry and Fe–N distances (see figure caption) are compatible only with a low-spin iron(III) state.[21] The intramolecular Fe–Cu distance is 6.0 Å. Also illustrated in Figure 1 is an *inter*molecular interaction of probable importance to magnetic coupling. There is a slipped, face-to-face relationship between adjacent copper chelates giving a linear chain of Cu–Fe–Cu units throughout the lattice. The interchelate mean plane spacing is 3.37 Å, and the intermolecular Cu···Cu separation is 4.13 Å.

The magnetic properties of the nickel(II) species $[Fe(TPP)(NiIm)_2]B_{11}CH_{12}\cdot 5THF$ are entirely typical of a low-spin $S = 1/2$ bis-imidazole iron(III) porphyrin. Field dependent Mossbauer data have been fit to a $(xy)^2(xz,yz)^3$ ground state with $g_x = 1.63$, $g_y = 2.14$ and $g_z = 2.90$. This leads to the fit of the susceptibility data shown in Figure 2a and is consistent with the EPR obtained in 1:1 toluene/acetone at 11 K ($g = 1.69$, 2.29, and 2.81). On the other hand, the magnetic properties of the copper(II) species $[Fe(TPP)(CuIm)_2]B_{11}CH_{12}$ reveal intramolecular ferromagnetic coupling. This is qualitatively seen in Figure 2b as an increase in magnetic moment with decreasing temperature, maximizing at about 10 K. The decrease in μ_{eff} below 10 K is ascribed to lattice antiferromagnetic coupling as suggested by the linear chain configuration of cations seen in the X-ray structure.[22] The data cannot be fit quantitatively by a standard isotropic $S = 1/2$, $S = 1/2$, $S = 1/2$ spin Hamiltonian. A satisfactory fit requires both an anisotropic treatment for iron[23] (using the g values of the Ni analogue) and a linear chain treatment[24] of the intermolecular coupling (rather than intramolecular coupling). The fit shown in Figure 2b is derived from a spin Hamiltonian of the form[25]

$$\mathbf{H} = \mathbf{H}_c + \mathbf{H}_m - \beta g_{Cu}\mathbf{H}_{ap}\cdot(\mathbf{S}_{Cu1} + \mathbf{S}_{Cu2}) - J_{FeCu}\mathbf{S}_{Fe}\cdot(\mathbf{S}_{Cu1} + \mathbf{S}_{Cu2})$$

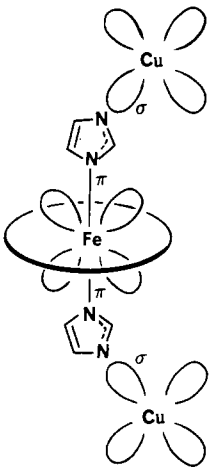

Figure 3. A schematic representation of the σ/π orthogonality of the magnetic orbitals, which rationalizes the *ferro*magnetic interaction.

The expectation value of the molecular magnetic moment obtained from this Hamiltonian is multiplied by a factor f where

$$f = [1 + U(K)]/[1 - U(K)]$$

$$U(K) = \coth(K) - 1/K$$

and

$$K = J/2kT$$

where J is Fisher's[24] normalized coupling constant. This gives rise to a value of $J_{FeCu} = +22$ cm^{-1} for the intramolecular coupling constant and a value of $J_{CuCu} = -1.9$ cm^{-1} for the intermolecular coupling constant. Temperature-dependent EPR studies are planned to augment this phenomenological description.

The magnitude of the intramolecular ferromagnetic interaction is quite large considering the large separation of the magnetic orbitals. The sign of the coupling constant is readily understood by inspection of the symmetries of the magnetic orbitals. The EPR results indicate that the unpaired electron on iron is in the d_{xz} (or d_{yz}) orbital, and this conclusion is consistent with the field-dependent Mossbauer studies. This orbital has π symmetry with respect to the iron–imidazolate bond. On the other hand, the tetragonal coordinate geometry at copper requires its unpaired electron to be in a $d_{x^2-y^2}$ type orbital which has σ symmetry with respect to the copper–imidazolate bond. This is illustrated in Figure 3. The π/σ orthogonality provides a ready explanation for a ferromagnetic interaction. Orthogonality of magnetic orbitals[14b] also underlies the weak ferromagnetic interaction between low-spin iron(III) and copper(II) in a related cyanide-bridged system.[26] It is a new observation for imidazolate and possibly a new observation for any bidentate N-heterocycle acting as a bridging ligand. It contrasts with the σ/σ pathway for overlap of magnetic orbitals available to all imidazolate complexes that show antiferromagnetic coupling.

Acknowledgment. We thank the National Institutes of Health for support through Grants GM-23851 to C.A.R., GM-38401 to W.R.S., HL-16860 to G.L. and the donors of the Petroleum Research Fund, administered by the American Chemical Society, for partial support of this research (G.A.B.).

Supplementary Material Available: Figures S1 and S2 illustrating the atom labeling scheme for the ruffled porphinato core and the axial coordination groups and Table SI, atomic coordinates, Table SII, anisotropic temperature factors, Table SIII, rigid

(20) $[Fe(TPP)(CuIm)_2]B_{11}CH_{12}\cdot 3DMF\cdot 3H_2O$ crystal data: $Cu_2FeCl_2O_8N_{15}C_{100}B_{11}H_{97}$; triclinic, $a = 14.403$ (8) Å, $b = 17.682$ (12) Å, $c = 21.577$ (12) Å, $\alpha = 76.58$ (5), $\beta = 73.54$ (5), $\chi = 84.80$ (5), $V = 5124.4$ Å^3, $Z = 2$, space group $P\bar{1}$, $\rho_{calcd} = 1.30$ g/cm^3; 5677 observed data to $2\theta = 45.8$ (graphite-monochromated Mo Kα radiation), all measurements at -155 ± 3C. Despite the use of low-temperature data collection methods, the number of observed data was limited by the small crystal sizes available. The structure was solved by a combination of the direct methods programs MULTAN78 and DIRDIF and refined by full-matrix least-squares methods to a current $R = 14.4\%$ with anisotropic temperature factors for seven atoms.

(21) Scheidt, W. R.; Reed, C. A. *Chem. Rev.* **1981**, *81*, 543.

(22) It is assumed that the intermolecular Cu···Cu interaction seen in the X-ray structure of the $3DMF\cdot 3H_2O$ solvate may also be present in the 5THF solvate on which the detailed Mossbauer and magnetic studies were done. Magnetic data on both solvates are closely comparable, and face-to-face ring stacking is likely in all lattices for these types of molecules.

(23) (a) Griffith, J. S. *Nature London* **1957**, *180*, 30. (b) Lang, G.; Marshall, W. *Proc. Phys. Soc.* **1966**, *87*, 3.

(24) Fisher, M. *Am. J. Phys.* **1964**, *32*, 343.

(25) $\mathbf{H}_c$ and $\mathbf{H}_m$ are the crystal field and Zeeman magnetic interaction terms, respectively. A value of $g_{Cu} = 2.12$ was derived from the difference in susceptibility of the Ni and Cu complexes.

(26) (a) Gunter, M. J.; Berry, K. J.; Murray, K. S. *J. Am. Chem. Soc.* **1984**, *106*, 4227. (b) Bencini, A.; Gatteschi, D.; Zanchini, C. *Mol. Phys.* **1985**, *56*, 97.

group parameters and derived crystallographic coordinates for the $B_{11}CH_{12}^-$ anion, and Tables SIV, SV, and SVI, magnetic susceptibility data for $Fe(TPP)(CuIm)_2 \cdot 2$toluene, $[Fe(TPP)(NiIm)_2]B_{11}CH_{12} \cdot 5THF$, and $[Fe(TPP)(CuIm_2)]B_{11}CH_{12} \cdot 5THF$, respectively (11 pages). Ordering information is given on any current masthead page.

Organometallic Vapor Phase Epitaxy of InP Layers Using the New Precursor Methylcyclopentadienylindium

Emiel G. J. Staring* and Gaby J. B. M. Meekes

Philips Research Laboratories, P.O. Box 80.000 5600 JA Eindhoven, The Netherlands

Received April 4, 1989

An important application of organometallic vapor phase epitaxy (OMVPE) is the growth of thin, monocrystalline layers of III–V semiconductor materials such as GaAs and InP for electronic and optoelectronic devices.[1-3] Basically the OMVPE growth of such III–V materials involves the thermal decomposition, in the gas phase, of a group III alkyl such as $In(CH_3)_3$ and a group V hydride such as PH_3 for the growth of InP (eq 1).

$$In(CH_3)_3 + PH_3 \xrightarrow[600\text{–}700\ °C]{H_2} InP + 3\ CH_4 \qquad (1)$$

OMVPE is chemically and technologically complicated, and the nature of the chemical reactions that occur in the gas phase and at the gas–solid interface is only poorly understood.

Some of the many problems encountered in epitaxial growth are the incorporation of residual carbon from the organometallic precursor[4] and unwanted prereactions or side reactions of group III and V compounds in the gas phase.[5,6] The effects of these side reactions in OMVPE are especially pronounced in the growth of In- and P-containing semiconductors,[2,7] and for a long time they prevented the growth of high quality InP by OMVPE. In these side reactions, the adduct **1** is in chemical equilibrium with $In(CH_3)_3$ and PH_3; **1** may also decompose, with elimination of CH_4, to produce the polymeric compound **2** (eq 2). The polymeric compound **2** may be, at least partially, responsible for the incorporation of carbon in the growing layer.

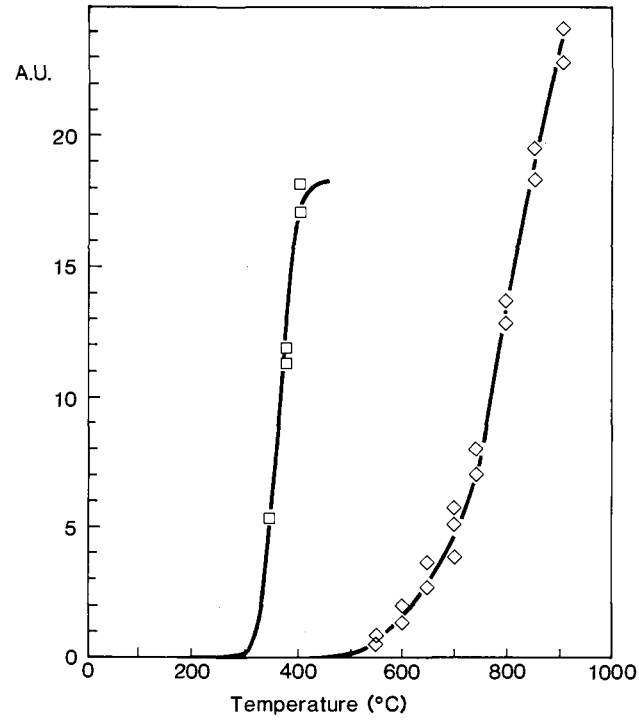

Figure 1. Thermal decomposition of $(CH_3C_5H_4)In$ (◇) and $(CH_3)_3In$ (□) in H_2 atmosphere. The amount of In metal deposited per unit time, normalized for the area of the substrate, is expressed as a rate in arbitrary units.

Table I. Vapor Pressure of CpIn Compounds and In Alkyls

indium compd	P_v (Pa) at 20 °C	P_v (Pa) at 40 °C
$(C_5H_5)In$	12	36
$(CH_3C_5H_4)In$	53	236
$(CH_3CH_2C_5H_4)In$	28	52
$(CH_3)_3In^a$	236	1040
$(CH_3CH_2)_3In^a$	13	145

[a] From ref 10.

$$n In(CH_3)_3 + n PH_3 \rightleftarrows \underset{\mathbf{1}}{n(CH_3)_3In\text{–}PH_3} \xrightarrow{-2nCH_4} \underset{\mathbf{2}}{\{(CH_3)In\text{–}PH\}_n} \qquad (2)$$

Several procedures have been suggested in literature[3,5,8-11] that diminish the deleterious effects of these side reactions in OMVPE. However, none of them removes the true cause of these side reactions: the Lewis acid character of the III alkyl and the Lewis base properties of the V hydride.

(1) For a recent review and an overview of the area, see: MRS Symposium Series No. 102, *Epitaxy of Semiconductor Layered Structures*; Tung, R. I., Dawson, L. R., Gunshor, R. L., Eds.; Materials Research Society: Pittsburgh, PA, 1987. Proceedings of the Tenth International Conference on Chemical Vapour Deposition, Cullen, G. W., Blocher, J. M., Jr., Eds.; The Electrochemical Society, Inc.: Pennington, NJ, 1987. Proceedings of the Fourth International Conference on Metal Organic Vapour Phase Epitaxy. *J. Cryst. Growth* **1988**, *93*, 1–940. Stringfellow, G. B. *Semiconductors and Semimetals*; Tsang, T. S., Ed.; Academic Press, Inc.: New York, 1985; Vol. 22, Part A, pp 209–259.

(2) Ludowise, M. J. *J. Appl. Phys.* **1985**, *58*, R31–R55.

(3) Razeghi, M. *Semiconductors and Semimetals*; Tsang, W. T. Ed.; Academic Press, Inc.: 1985; Vol. 22 part A, pp 299–378.

(4) Lum, R. M.; Klingert, J. K.; Kisker, D. W.; Abys, S. M.; Stevie, F. A. *J. Cryst. Growth* **1988**, *93*, 120–126. Aina, O.; Mattingly, M.; Steinhauser, S.; Mariella, R., Jr.; Melas, A. *J. Cryst. Growth* **1988**, *92*, 215–221.

(5) Bass, S. J.; Pickering, C.; Young, M. L. *J. Cryst. Growth* **1983**, *64*, 68–75. Ludowise, M. J.; Cooper, III, C. B.; Saxena, R. R. *J. Electron. Mat.* **1981**, *10*, 1051–1068. Cooper, III, C. B.; Ludowise, M. J.; Aebi, V.; Moon, R. L. *J. Electron. Mat.* **1980**, *9*, 299–309. Hallais, J. P. *Acta Electron.* **1978**, *21*, 129–138. Duchemin, J. P.; Bonnet, M.; Beuchet, G.; Koelsch, F. *Inst. Phys. Conf. Ser.* **1979**, *45*, 10.

(6) For similar reactions of group III and V compounds, see: Harrison, B. C.; Tompkins, E. H. *Inorg. Chem.* **1962**, *1*, 951–953. Beachley, O. T.; Coates, G. E. *J. Chem. Soc.* **1965**, 3241. Pitt, C. G.; Higa, K. T.; McPhail, A. T.; Wells, R. L. *Inorg. Chem.* **1986**, *25*, 2483–2484. Arif, A. M.; Benac, B. L.; Cowley, A. H.; Geerts; R.; Jones, R. A.; Kidd, K. B.; Power, J. M.; Schwab, S. T. *J. Chem. Soc., Chem. Commun.* **1986**, 1543–1545. Pitt, C. G.; Purdey, A. P.; Higa, K. T.; Wells, R. L. *Organometallics* **1986**, *5*, 1266–1268. Beachley, O. T., Jr.; Kopasz, J. P.; Zhang, H.; Hunter, W. E.; Atwood, J. L. *J. Organomet. Chem.* **1987**, *325*, 69–81.

(7) Kuo, C. P.; Cohen, R. M.; Stringfellow, G. B. *J. Cryst. Growth* **1983**, *64*, 461–470. Stringfellow, G. B. *J. Cryst. Growth* **1984**, *68*, 111–122.

(8) Duchemin, J. P. *J. Cryst. Growth* **1981**, *55*, 64–73. Benz, K. W.; Renz, H.; Weidlein, J.; Pilkuhn, M. H. *J. Electron. Mat.* **1981**, *10*, 185–192. Renz, H.; Weidlein, J.; Benz, K. W.; Pilkuhn, M. H. *Electron. Lett.* **1980**, *16*, 228. Maury, F.; Constant, G. *J. Cryst. Growth* **1984**, *68*, 88–95. Maury, F.; Constant, G. *Polyhedron* **1984**, *3*, 581–584. Duchemin, J. P. *J. Vac. Sci. Technol.* **1981**, *18*, 753–755.

(9) Cowley, A. H.; Benac, B. L.; Ekerdt, J. G.; Jones, R. A.; Kidd, K. B.; Lee, J. Y.; Miller, J. E. *J. Am. Chem. Soc.* **1988**, *110*, 6248–6249. Schumann, H.; Hartmann, U.; Dietrich, A.; Pickardt, J. P. *Angew. Chem.* **1988**, *100*, 1119–1120. Bradley, D. C.; Faktor, M. M.; Scott, M.; White, E. A. D. *J. Cryst. Growth* **1986**, *75*, 101–106. Reier, F. W.; Wolfram, P.; Schumann, H. *J. Cryst. Growth* **1986**, *77*, 23–26. Byrne, E. K.; Parkanyi, L.; Theopold, K. H. *Science* **1988**, *241*, 332–334. Maury, F.; Combes, M.; Constant, G.; Carles, R.; Renucci, J. B. *J. Physique* **1982**, *43C1*, 347–352. Zaouk, A.; Salvetat, E.; Sakaya, J.; Maury, F.; Constant, G. *J. Cryst. Growth* **1981**, *55*, 135–144.

(10) Bass, S. J.; Skolnick, M. S.; Chudzynska, H.; Smith, J. *J. Cryst. Growth* **1986**, *75*, 221–226. Moss, R. H. *J. Cryst. Growth* **1984**, *68*, 78–87.

(11) Bradley, D. C.; Faktor, M. M.; Frigo, D. M.; Smith, L. M. *J. Cryst. Growth* **1988**, *92*, 37–45. Bradley, D. C.; Faktor, M. M.; Frigo, D. M.; Young, K. V. *Chemtronics* **1988**, *3*, 50–52.

0002-7863/89/1511-7648$01.50/0